NeuroMolecular Medicine (2019) 21:401–413
https://doi.org/10.1007/s12017-019-08557-3

ORIGINAL PAPER

Altered Hippocampal–Prefrontal Dynamics Following Medial Prefrontal Stroke in Mouse

Kristin L. Hillman[1] · Hannah J. Wall[1] · Luke O. Matthews[1] · Emma K. Gowing[2] · Andrew N. Clarkson[2]

Received: 9 April 2019 / Accepted: 12 July 2019 / Published online: 16 July 2019

Abstract

Frontal infarcts can produce cognitive impairments that affect an individual's ability to function in everyday life. However, the precise types of deficits, and their underlying mechanisms, are not well-understood. Here we used a prefrontal photothrombotic stroke model in C57BL/6*J* mice to characterise specific cognitive changes that occur in the 6 weeks post-stroke. Behavioural experiments were paired with in vivo electrophysiology to assess whether changes in oscillatory communication between the prefrontal cortex (PFC) and the hippocampus (HPC) mirrored any observed behavioural changes. We found that mice in the stroke group exhibited a delayed onset impairment in tasks of spatial working memory (object location recognition and Y-maze) and that this correlated with reduced PFC–HPC theta band coherence (5–12 Hz) during the task. In the open field, mice in the stroke group exhibited hyperactivity as compared to controls, and stroke animals also exhibited significantly higher beta band activity (13–30 Hz) in the PFC and the HPC. Taken together our results suggest that infarcts in the PFC result in PFC–HPC oscillatory communication changes in the theta and beta bands, correlating with altered performance in spatial memory and open field tasks respectively. Of particular interest, early open field changes in PFC beta band power post-stroke correlated to later-stage spatial memory impairments, highlighting this as a potential biomarker for detecting when spatial memory impairments are likely to occur.

Keywords Spatial memory · Prefrontal · Coherence · Photothrombotic stroke · Theta · Beta

Introduction

Strokes that affect the prefrontal cortex (PFC) or its relevant circuitry can cause cognitive deficits and post-stroke depression (Moorhouse and Rockwood 2008; Rodriguez Garcia and Rodriguez Garcia 2015; Vahid-Ansari et al. 2016). While these deficits are a major contributor towards long-term morbidity (Levine et al. 2015; Patel et al. 2002; Tatemichi et al. 1994), they may escape clinical detection for a number of reasons. For one, PFC infarct-related impairments can be difficult to detect in patients with existing pre-stroke Mild Cognitive Impairment (Moorhouse and Rockwood 2008; Petersen 2004). Secondly, diagnostic criteria for vascular cognitive dysfunction have long been biased towards detecting memory deficits, when problems with executive function and spatial reasoning are often more pronounced (O'Brien et al. 2003; Rodriguez Garcia and Rodriguez Garcia 2015; cf. Hachinski et al. 2006). Thirdly, post-stroke cognitive dysfunction may exhibit a delayed onset which falls outside of clinical observation and reporting periods (Levine et al. 2015; Patel et al. 2002; Tatemichi et al. 1994). Adequately characterising PFC infarct-related cognitive dysfunction, and/or identifying clinical indicators that cognitive dysfunction is likely to develop over a projected time course, remain important outstanding questions in the field.

Cognitive dysfunction following prefrontal ischemia is not surprising given the significant role played by the PFC in executive function and cognitive control. Rodent models have demonstrated post-stroke executive dysfunction in attentional set shifting, decision-making and behavioural perseveration (Cordova et al. 2014; Deziel et al. 2015; Endepols et al. 2015; Livingston-Thomas et al. 2015). Changes in object recognition abilities following prefrontal ischemia

✉ Andrew N. Clarkson
andrew.clarkson@otago.ac.nz

[1] Department of Psychology, University of Otago, PO Box 56, Dunedin 9054, New Zealand

[2] Department of Anatomy, Brain Health Research Centre and Brain Research New Zealand, University of Otago, PO Box 56, Dunedin 9054, New Zealand

are inconsistent in the literature, with some studies reporting deficits in a variety of object recognition tests (Livingston-Thomas et al. 2015) and others finding no significant differences between stroke and sham animals (Deziel et al. 2015; Zhou et al. 2016). Likewise, post-stroke anxiety measures in the elevated plus maze and open field are elevated in some studies (Vahid-Ansari and Albert 2018; Vahid-Ansari et al. 2016) and significantly reduced in others (Endepols et al. 2015; Hewlett et al. 2014). Inconsistencies may stem from differences in lesion location and size, but also from differences in the post-stroke time points examined (e.g. post-stroke day 7 vs day 42) and differences in task design (e.g. inter-trial interval (ITI) times of 2 min vs 1 h). It would be informative to characterise performance within the same task across the post-stroke time course to better delineate when and how cognitive dysfunctions emerge.

Post-stroke deficits in spatial memory—a function usually ascribed to the hippocampus (HPC)—have also been reported in rodent models of prefrontal ischemia. Deficits in spatial Y-maze alternation and Morris Water Maze performance have been reported (Endepols et al. 2015; Hewlett et al. 2014; Vahid-Ansari and Albert 2018), as well as deficits in object location recognition (OLR) tasks (Livingston-Thomas et al. 2015; Zhou et al. 2016). However inconsistencies between studies are also seen with spatial memory task performance; as mentioned above, examining these tasks across the post-stroke time course, within the same cohort, may provide better behavioural phenotyping and mechanistic insight.

One possible mechanism underlying the cognitive dysfunctions seen post-stroke is altered oscillatory communication between the PFC and HPC. The PFC and HPC are reciprocally connected mono-synaptically as well as di-synaptically via the ventral midline thalamic nuclei (Griffin 2015). Functional PFC–HPC communication, notably in the theta band, is important for spatial working memory tasks (Benchenane et al. 2010; Hyman et al. 2010; Jones and Wilson 2005; O'Neill et al. 2013). Alterations in PFC–HPC oscillatory dynamics, intra- or inter-regionally, could underlie some of the performance deficits seen post-stroke. Here we used a PFC photothrombotic stroke model in C57BL/6*J* mice to determine: (1) the post-stroke time course of behavioural changes in four standard laboratory tasks, and (2) whether PFC infarct induces changes in PFC–HPC oscillatory dynamics post-stroke.

Materials and Methods

Subjects

Three cohorts of male C57BL/6*J* mice (5 months of age at start of study, 25–35 g) were used for the study. All experimental protocols were approved by the University of Otago Animal Ethics Committee (AEC Protocol 13/15), and procedures carried out in accordance with the ARRIVE guidelines. Mice were individually housed under a 12-h light–dark cycle; experimentation occurred during the light phase. Animals had ad libitum access to food and water. Mice were handled, habituated and trained in the experimental apparatuses for 2 months prior to the start of the study. During this time, they were also habituated to food reward (sesame seeds and sucrose discs). At the start of the study—Week 0—mice were block randomised into stroke animals or sham animals by Experimenter 1. Mice were then baseline tested in the behavioural tasks by Experimenters 2 and 3. At the end of Week 0, Experimenter 1 performed the surgeries. Cohort 1 ($n = 15$; 8 stroke and 7 sham) and cohort 2 ($n = 21$; 10 stroke and 11 sham) underwent stroke-only surgery. Cohort 3 ($n = 12$; 7 stroke and 5 sham) underwent stroke + electrode implant surgery. Cohorts 1 and 2 were used for behavioural phenotyping. Following surgery these mice underwent 6 weeks of behavioural testing, with subsets of mice perfused at Weeks (Wks) 2, 4 and 6 and brains processed for histological assessment of stroke volume. Subsets of mice were perfused at Wks 2, 4 and 6 post-stroke to assess if there is a progressive loss of cells in regions linked to the PFC, which is part of a larger ongoing study; these data are not reported here. Cohort 3 underwent stroke + electrode implant surgery, followed by 6 weeks of behavioural testing. Local field potentials (LFPs) were recorded from PFC and HPC during these behavioural testing sessions. After Wk 6 all mice were perfused and brains processed for histological assessment of stroke volume and electrode locations.

Surgical Procedure: Stroke Only

For cohorts 1 and 2, a bilateral photothrombotic stroke was induced in the mPFC as previously described (Zhou et al. 2016; Houlton et al. 2019). Briefly, the animal was anesthetised with isoflurane and mounted in a stereotaxic frame. The skull was exposed and Rose Bengal (Sigma, 2 mg in 0.2 ml sterile saline) was injected intraperitoneally and allowed to infuse for 5 min. A cold light source (Zeiss, KL1500 LCD) with 2-mm-diameter illumination was then positioned + 1.2 mm anterior to bregma and illuminated for 22 min. Sham animals underwent an identical procedure using 0.2 ml saline in lieu of the Rose Bengal. Following illumination the incision was closed and the animal was administered temgesic (0.003 mg subcutaneous) and monitored closely for five post-operative days. Five mice (three stroke mice, two sham mice) developed tail necrosis in the first 2 weeks post-stroke. It is unknown why tail necrosis developed after the surgical procedure; empirical investigations to-date (e.g. heat pad settings, holding room humidity) have been inconclusive.

Surgical Procedure: Stroke + Electrode Implant

For cohort 3, mice were first anaesthetised with isoflurane and a bilateral phothrombotic stroke (or saline sham) was induced as described above. After 22 min of illumination the light was removed and two nichrome unipolar electrodes were implanted via stereotaxic-guided craniotomy as previously described (Hillman and Bilkey 2010). From bregma, coordinates for mPFC were + 1.7 AP, 0.4 ML, − 1.5 DV; coordinates for dorsal HPC were − 1.9 AP, 1.5 ML, − 1.4 DV (Franklin and Paxinos 2008). All implants were unilateral right hemisphere. Electrodes were mounted in a McIntyre miniconnector headplug and a ground connection was soldered to a screw over the cerebellum; each electrode was referenced to this cerebellar ground connection for capture of LFPs during the testing tasks. The assembly was secured using modified skull screws and dental cement (3 M, Transbond). Mice were subcutaneously administered pre- and post-operative amphoprim (0.9 mg) and carprieve (0.15 mg), plus one dose of temgesic (0.003 mg) immediately after anaesthesia. Mice were monitored closely for 7 post-operative days. Two stroke animals died within the first week, and one sham animal was perfused early in the 6th week after loss of its headplug.

Behavioural Testing

Four tasks were used: an open field (OF) task, a novel object recognition (NOR) task, an OLR task, and a Y-maze task. Each task was conducted on its own day, with the four tasks being carried out across four consecutive days. Each mouse was individually tested on the task pre-stroke to provide a baseline measure (Wk 0), with testing then repeated at post-stroke Wks 2, 4 and 6. For all behavioural tasks in the stroke-only cohorts, overhead video tracking software (Noldus, EthoVision) was used to track the mouse's movement, with specific behaviours of interest being manually key coded by the experimenter blind as to the surgical intervention (stroke vs sham). For the stroke + electrode implant cohort, movement and behaviours of interest were tracked via the electrophysiological data acquisition system, described below.

For the OF task mice were placed in a circular arena (1 m diameter, 35 cm walls) and allowed to explore the arena for 10 min. Distance travelled and thigmotaxis were measured; the latter was scored as being within 15 cm of the arena wall. For the NOR task mice were placed in a rectangular arena (60 × 37 × 25 cm) containing two object zones (Zone A and Zone B, each 15 × 15 cm); each object zone initially contained an identical small novelty-store object. Mice were given three 10-min sessions in the arena at 60-min intervals. In the third session (test phase), the object in Zone B was replaced with a new novelty-store object. Novel object exploration time was calculated as a percentage: (time spent exploring B)/(time spent exploring A + B). Object exploration was defined as the mouse being within 2 cm of the object and oriented towards the object.

The OLR task used the same arena and ITI scheduling as the NOR task. However in the OLR task, all three sessions utilised the same pair of identical small novelty-store objects, with the third session (test phase) involving a spatial location shift. The object in Zone B was shifted to the adjacent quadrant of the arena, Zone C. Object relocation exploration time was calculated as a percentage: (time spent exploring C)/(time spent exploring A + C). For the OLR and NOR tasks, different sets of objects were utilised at each time point, i.e. the objects in OLR Wk 2 differed from those used in OLR Wk 0, the objects used in OLR Wk 4 differed from those used in OLR Wk 2 and so on. The sets of objects used for the NOR task were different than those used for the OLR task.

For the Y-maze task, mice were placed in a start zone at the base of a Y-maze (40 × 6.5 × 13 cm for each arm). They then ran ten trials of a delayed non-match to sample task as described by O'Neill et al. (2013). In the 'Sample' phase of each trial, one arm was blocked and the animal needed to travel down the unblocked arm and return to start. After a 10 s delay the animal was then given a 'Choice' phase where both arms were unblocked. To earn a reward the animal needed to travel down the previously blocked arm. The ITI was 20 s.

LFP Data Collection

Neural data were acquired and recorded using a Cheetah acquisition system (Neuralynx). Neural data were sampled at 5 kHz and filtered 0.1–500 Hz. Tracking data, collected via headstage mounted LEDs, was sampled at 25 Hz. Data were processed offline in MATLAB using Neuralynx's NLx-2Mat file unpacking scripts and custom analysis scripts. LFP recordings were down-sampled to 500 Hz and notch-filtered to remove 50 Hz noise. The signal was then segmented in preparation for analysis. For the OF, NOR and OLR tasks, the first 120 s of signal was used, representing the first 2 min that the animal was in the task apparatus. For the Y-maze task, a spatial region-of-interest was first set around the base arm of the Y-maze, up to and including the Y choice juncture, and excluding the 8 cm start zone area. A south-to-north travel specifier was then set, corresponding to when the animal ran from the start zone up to and within the Y choice juncture point (i.e. excluding travel in the region-of-interest that was part of the 'return trip' back to the start zone). Together this allowed us to form a concatenated signal representative of the time the animal was travelling from the start zone up to and within the Y choice juncture. Mean duration (± SD) of the resultant signal was 36 ± 4 s. For all task signals, frequency bands of interest

were set as theta 5–12 Hz and beta 13–30 Hz; a broad spectrum band (2–90 Hz) was also set for calculation of relative power. Power spectral densities were computed using a modified *pwelch* function; relative power was calculated as power in the band of interest divided by broad spectrum power. LFP–LFP coherence was calculated using a modified *mscohere* function. Data outputs were transferred into GraphPad 7.04 (Prism) for statistical analysis and graphing. Behavioural differences between groups across time were assessed using two-way ANOVA with post-hoc Sidak's multiple comparisons. Electrophysiological differences between groups across frequency bands were assessed using the same tests. For all analyses significance was set as $p < 0.05$.

Histology

Mice were perfused at either post-stroke Wk 2, 4 or 6, after behavioural tasks for that week were completed; these staggered perfusions were for the purpose of a larger, ongoing immunohistochemistry project (data not reported here). Deep anaesthetization was induced via intraperitoneal pentobarbital (100 mg/kg) and mice were transcardially perfused with 4% PFA in 0.1 M phosphate buffer. After 24 h brains were transferred to 30% sucrose in PBS and stored at 4 °C until sectioning. Brains were sectioned at 30 µm on a freezing microtome and mounted on gelatine coated slides from free floating 10 × TBS. Stroke volume and electrode placements were assessed using standard cresyl-violet staining and Image J (NIH). Electrode locations were assessed by comparing slides with coronal images from the mouse brain atlas (Franklin and Paxinos 2008).

Results

Stroke Volume and Electrode Placements

The photothrombotic technique induced a medial infarct that was consistent with previously published findings (Zhou et al. 2016; Houlton et al. 2019); the majority of stroke volume spanned + 1.0 to + 1.9 anterior of bregma, affecting cingulate and secondary motor area. Consistent with what we have reported previously, we did not observe any tissue damage in any of the sham animals (Zhou et al. 2016; Houlton et al. 2019). Two animals in the original stroke group were excluded from all analyses; one animal had inadequate infarct volume (< 0.50 mm^3) and the other was a statistical outlier (7.7 mm^3). Mean stroke volume across remaining animals was 2.6 ± 1.1 mm^3 overall; there was no difference in mean stroke volume across the weeks examined ($F(2,18) = 0.35$, $p = 0.71$; Fig. 1a). For animals with electrode implants, electrode locations were checked by cresyl-violet staining at the end of the study (Fig. 1b). Three animals' data—two stroke and one sham—were excluded from subsequent electrophysiological analysis due to incorrect or unconfirmed electrode placements; behavioural data from these animals were still included in the behavioural analysis. When animal deaths and all exclusions mentioned above were accounted for, the resulting group sizes (stroke:sham)

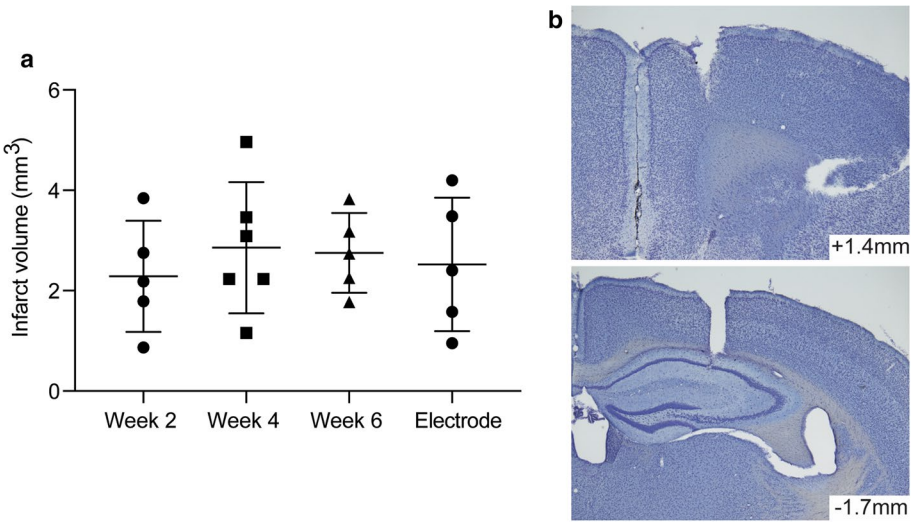

Fig. 1 Stroke volume and electrode placements. **a** Stroke volumes for the 21 stroke animals used for analysis are shown here, segregated by collection weeks (Weeks 2, 4 and 6 for the non-implanted group, and Week 6 for the electrode implanted group). Mean ± SD indicated over individual data points. **b** Representative sections from a sham animal indicating electrode placements; this animal was scored as having mediocre placements, with electrodes falling slightly outside of target coordinates. Distance (mm) from bregma given anterior/posterior. Three animals were scored as having poor placements, and these were excluded from all electrophysiological analysis

for the behavioural experiments were 21:23 for Wk 2, 16:17 for Wk 4, and 10:11 for Wk 6. For the electrophysiological experiments, the resulting group size (stroke:sham) was 3:4 for all 6 weeks.

Open Field (OF)

In the non-implanted mice, prior to stroke surgery, there were no differences between the stroke and sham animal groups in the OF with regard to distance travelled ($p = 0.69$) or thigmotaxis ($p = 0.29$, unpaired t test; data not shown). After stroke surgery, there was a significant main effect of Group on distance travelled ($F(1, 62) = 9.8$, $p = 0.003$). Stroke animals travelled more distance as compared to shams, notably in Wk 4 ($p = 0.01$, Sidak's multiple comparisons; Fig. 2a). There was no main effect of Time or Group × Time interaction. Thigmotaxis did not differ between groups, $F(1,62) = 0.8$, $p = 0.37$.

In the implanted mice, there was a significant main effect of Group on distance travelled, again with stroke mice covering more distance overall as compared to shams ($F(1, 15) = 5.1$, $p = 0.04$; Fig. 2b). There was no main effect of Time or Group × Time interaction. Thigmotaxis did not differ between groups, $F(1,15) = 0.82$, $p = 0.38$. Relative theta power in the PFC and HPC—and theta coherence between PFC and HPC—did not differ between groups, or across the time course (all $p \geq 0.33$; Fig. 2c). However, differences in the beta band were observed (Fig. 2d). Stroke animals had significantly more localised beta oscillatory activity in the PFC ($F(1,15) = 5.8$, $p = 0.03$) and in the HPC ($F(1,15) = 6.3$, $p = 0.02$) as compared to shams. Beta band PFC–HPC coherence was also elevated in the stroke animals ($F(1,15) = 12.6$, $p = 0.003$).

Novel Object Recognition (NOR)

In the non-implanted mice, prior to stroke surgery, there were no differences between the stroke and sham animal groups in the NOR task with regard to percent time exploring the novel object ($p = 0.44$, unpaired t test). After stroke surgery, there were no significant behavioural effects seen in this task, either between Groups ($F(1,62) = 1.2$, $p = 0.27$) or across Time ($F(2,62) = 1.56$, $p = 0.22$; Fig. 3a). These behavioural results were replicated in the implanted mice; there was no main effect of Group ($F(1,15) = 0$, $p > 0.99$; Fig. 3b) or Time ($F(2,15) = 0.41$, $p = 0.67$). Electrophysiological recordings were unremarkable overall; data not shown. There were no significant main effects of Group or Time on prefrontal power (relative θ $p = 0.37$, β $p = 0.28$), hippocampal power (relative θ $p = 0.65$, β $p = 0.53$), or PFC–HPC coherence during the task (θ $p = 0.49$, β $p = .86$).

Object Location Recognition (OLR)

In the non-implanted mice, prior to stroke surgery, there were no differences between the stroke and sham animal groups in the OLR task with regard to percent time exploring the relocated object ($p = 0.56$, unpaired t test). After stroke surgery, there was a significant main effect of Group ($F(1, 62) = 12.96$, $p < 0.001$). Stroke animals spent less time exploring the relocated object as compared to shams, notably in Wks 2 and 4 ($p = 0.002$ and $p = 0.03$ respectively, Sidak's; Fig. 4a). There was no main effect of Time or Group × Time interaction.

In the implanted mice, there was also a significant main effect of Group in the OLR task ($F(1, 15) = 10.3$, $p = 0.006$; Fig. 4b). Stroke mice spent less time exploring the relocated object, notably in Wk 4 ($p = 0.03$). There was no significant group difference noted in Wk 2 as there had been for the non-implanted groups shown in Fig. 4a. This discrepancy between Fig. 4a and b is likely due to the small sample size of the implanted cohort ($n = 3$ stroke and $n = 4$ sham), combined with a particular animal's performance in the stroke group (95% exploration of the displaced object). Exploration values for the other two stroke animals in the task were 50 and 60%, whereas exploration values for the four sham animals were 52, 71, 79 and 82%.

In the implanted mice, there was no main effect of Time or Group × Time interaction in the OLR task. Relative theta power in the PFC and in the HPC did not differ between groups or across time (all $p \geq 0.11$); however, stroke animals exhibited reduced PFC–HPC theta coherence overall in the OLR as compared to shams ($F(1,15) = 4.87$, $p = 0.04$; Fig. 4c). Localised prefrontal beta power was higher in sham animals as compared to stroke animals ($F(1,15) = 9.8$, $p = 0.007$), and shams also exhibited increased PFC–HPC beta coherence ($F(1,15) = 8.6$, $p = 0.01$; Fig. 4d).

Y-Maze Task

In the non-implanted mice, prior to stroke surgery, there were no differences between the stroke and sham animal groups observed in Y maze task performance ($p = 0.76$, unpaired t test). After stroke surgery, there was no main effect of Time or Group × Time interaction. There was no overall main effect of Group ($F(1, 62) = 1.46$, $p = 0.23$); however, post-hoc multiple comparisons revealed a performance deficit in stroke animals in Wk 4 ($p = 0.04$, Sidak's; Fig. 5a). We conducted post-hoc tests—despite the lack of a main Group effect—based on a priori hypotheses that animals in the stroke group would exhibit delayed onset cognitive impairment at a specific time point. Previous work in our lab (Zhou et al. 2016) has demonstrated a spatial memory impairment in mice in post-stroke Wk 4 but not Wk 1, whereas rat work by others (Livingston-Thomas et al. 2015)

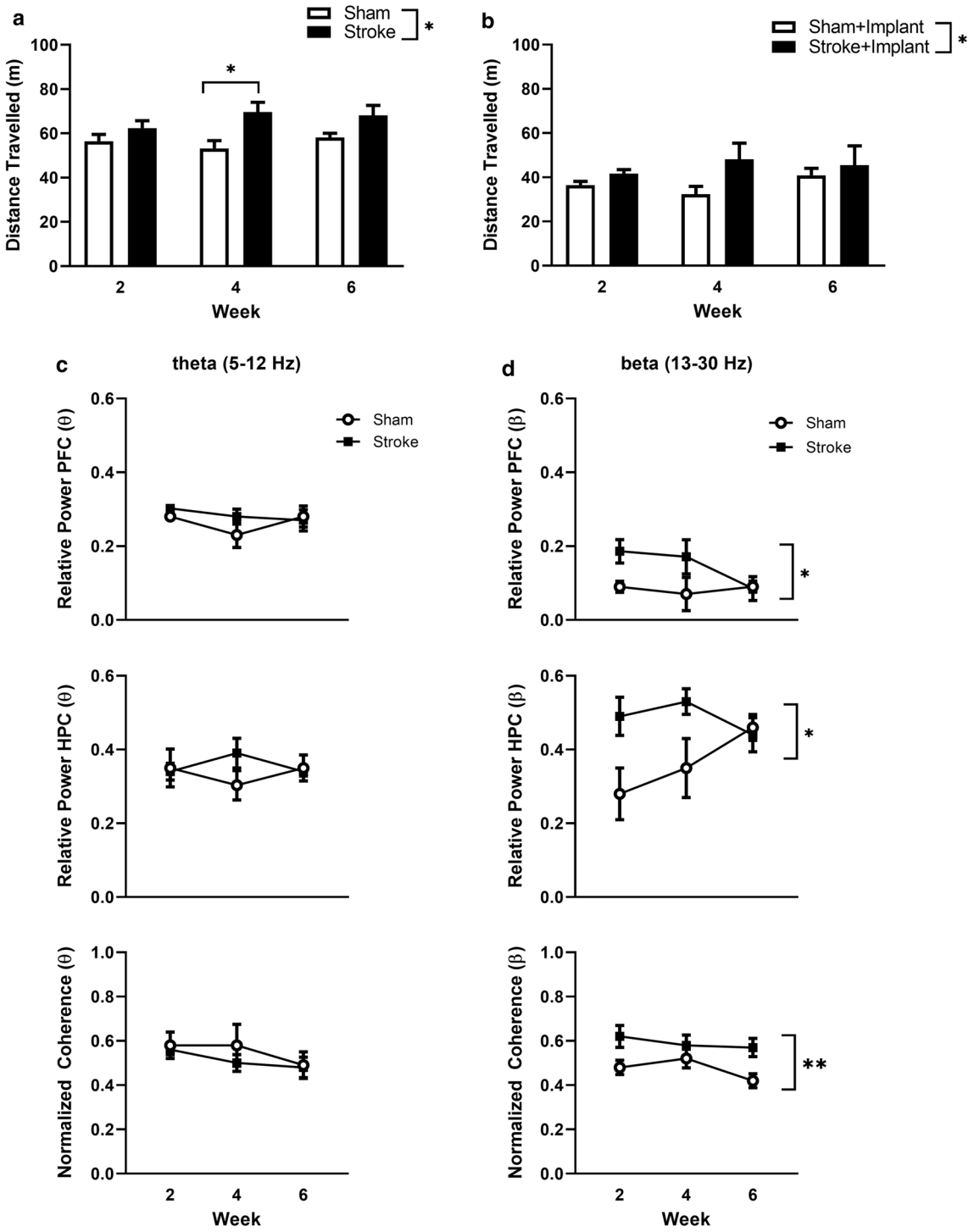

Fig. 2 Open field task. Behavioural data for **a** non-implanted animals and **b** electrode implanted animals. **c** Localised theta power in the PFC and HPC did not differ between groups or across time; coherence was also no different. **d** Localised beta power was higher in the PFC and HPC following prefrontal stroke; beta band coherence was also elevated in the stroke animals as compared to shams. Data are shown as mean ± SEM

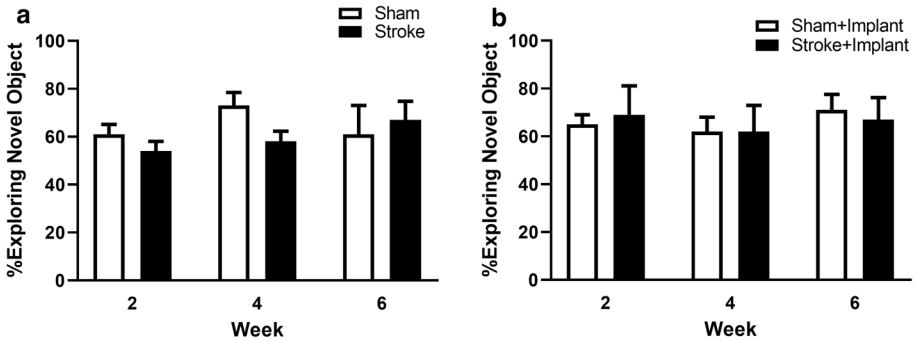

Fig. 3 Novel object recognition (NOR) task. Behavioural data for **a** non-implanted animals and **b** electrode implanted animals. Data are shown as mean ± SEM

has shown some performance deficits in Wks 3–4 but then no spatial deficit in Wks 7–18. Thus, an overall main effect of Group was not necessarily predicted in our study across the 6 weeks of testing.

In the implanted mice, there was a significant Group × Time interaction, $F(2,15) = 6.5$, $p = 0.009$. From Wks 2 to 4, sham animals' performance increased while stroke animals' performance decreased (Fig. 5b). Stroke animals were significantly impaired in the task in Wk 4 as compared to shams ($p = 0.001$, Sidak's). Relative theta power in the PFC and HPC did not differ between groups or across time (all $p \geq 0.21$); however, stroke animals exhibited reduced PFC–HPC theta coherence overall in the Y-maze task as compared to shams ($F(1,15) = 5.1$, $p = 0.04$; Fig. 5c). There were no significant changes in the beta band between group or across time (all $p \geq 0.26$, Fig. 5d).

Coherence Behaviour Correlation

To determine whether PFC–HPC coherence is associated with task performance, we used the individual data points from each implanted mouse ($n = 7$) to perform pair-wise correlations for tasks where significant changes in behaviour and/or electrophysiology were observed: the OF, OLR task and Y-maze task. Pearson's correlations revealed significant relationships in the OLR and Y-maze (Table 1). In the OLR, increased theta and beta band coherence between the PFC and HPC was associated with increased exploration of the displaced object in Wks 4 and 6. Likewise in the Y-maze, higher PFC–HPC theta coherence in Wks 4 and 6 was associated with correct choice performance in the delayed non-match to sample task. Additionally, higher beta band coherence in Wk 2 in the Y-maze was associated with worse performance in the task that week.

PFC–HPC coherence captured during the OF—either in the theta or beta band—did not correlate with distance travelled in the OF. However, we were curious if the elevated regional beta power observed post-stroke in both regions (see Fig. 2) was of any behavioural relevance. Of note, prefrontal beta power measured in Wk 2 was predictive of poor performance in the Y-maze in Wk 4 ($r - 0.78$, $p = 0.04$), poor performance in the OLR in Wk 4 ($r - 0.82$, $p = 0.03$), and increased locomotor activity in the OF in Wk 4 (r 0.77, $p = 0.04$). No significant correlations were observed between Wk 2 prefrontal beta power and Wk 6 performance measures, nor between Wk 2 hippocampal beta power and any behavioural measure. While highly preliminary at this stage, this suggests that prefrontal beta band activity changes may serve as an early indicator of future spatial memory impairments. Validation with a larger n, alongside studies of the inhibitory/excitatory neurotransmitter alterations occurring during this time period, will help to elucidate the physiological relevance of this beta power-based correlation.

Discussion

Cerebral ischemia to regions of the frontal cortex are generally not associated with overt sensorimotor deficits; however, they can produce cognitive-behavioural deficits that limit recovery and long-term psychosocial function (Vermeer et al. 2007). The exact time course of these cognitive-behavioural impairments, and the underlying mechanisms, remain ill-understood. Specific deficits in behavioural flexibility and spatial working memory have been reported in patients (Loeb et al. 1992; Tatemichi et al. 1994), and these have been reproduced in preclinical animal stroke models targeting the PFC (Cordova et al. 2014; Endepols et al. 2015; Livingston-Thomas et al. 2015; Zhou et al. 2016), albeit with some inconsistency. Much of the inconsistency likely stems from variable post-stroke time points being examined, and the different in-task parameters used between labs (e.g. ITIs). The former is particularly salient as post-stroke cognitive-behavioural impairments can exhibit a delayed onset (Zhou et al. 2016); hence, data captured early after a stroke may show no impairment.

Here we used a photothrombotic PFC stroke model in C57BL/6*J* mice to phenotype-specific cognitive-behavioural and electrophysiological changes occurring in the 6 weeks following prefrontal stroke. We predicted that the insult would cause impaired performance in two tests of spatial memory (OLR and Y-maze) and that this would

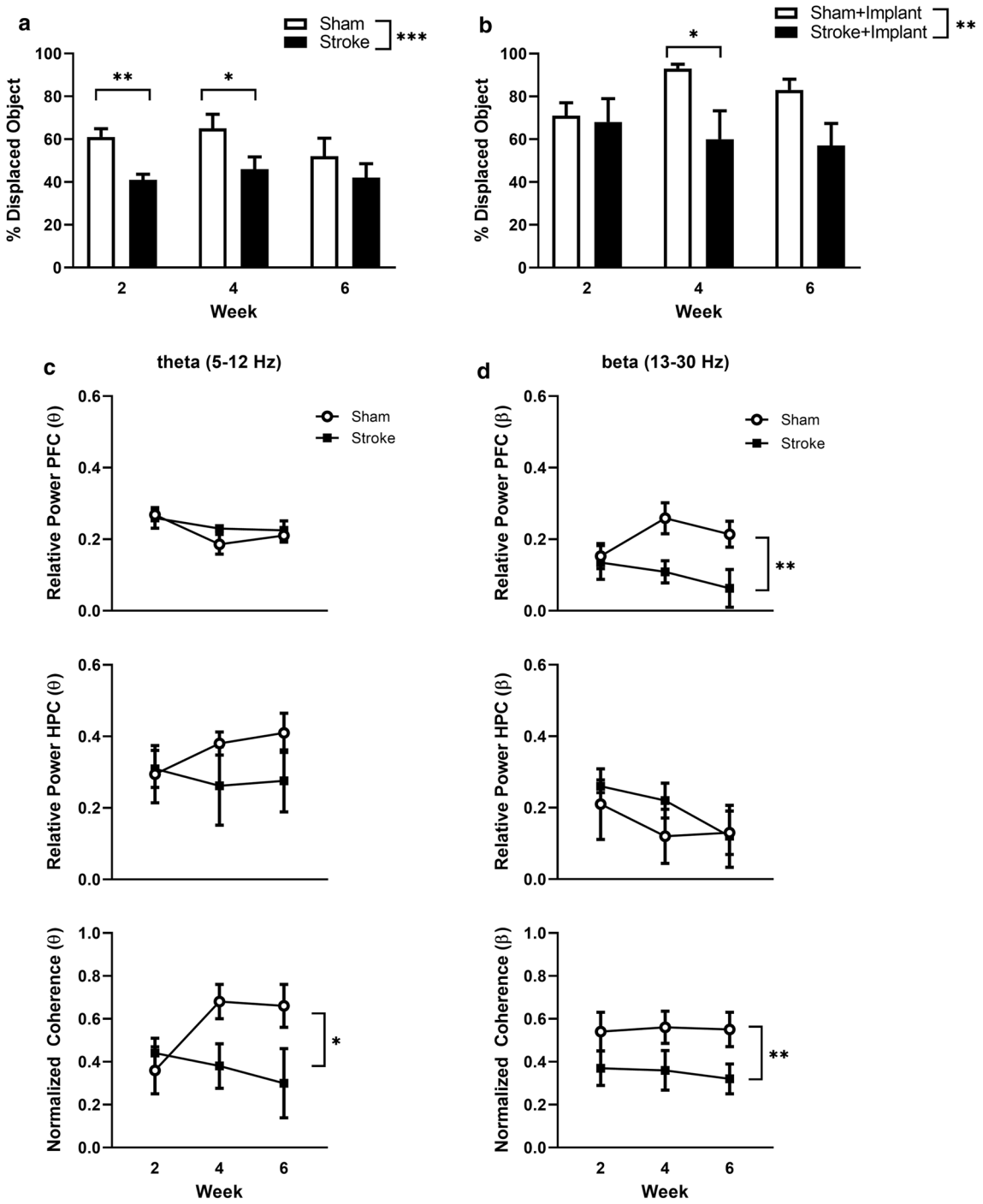

Fig. 4 Object location recognition (OLR) task. Behavioural data for **a** non-implanted animals and **b** electrode implanted animals. **c** Localised theta power in the PFC and HPC did not differ between groups or across time; however, theta coherence between the two regions was significantly less in the stroke animals. **d** Localised prefrontal beta power was higher in the sham animals overall, as was PFC–HPC beta coherence. Data are shown as mean ± SEM

coincide with aberrant oscillatory coherence between the PFC and HPC, two regions known to functionally interact during memory tasks (Colgin 2011). We focused our electrophysiological analysis on the theta and beta bands, as prefrontal–hippocampal synchronization in these bands is observed in spatial working memory, memory load and associative learning (Hyman et al. 2010; Jones and Wilson 2005; O'Neill et al. 2013; Brincat and Miller 2015; Lundqvist et al. 2016).

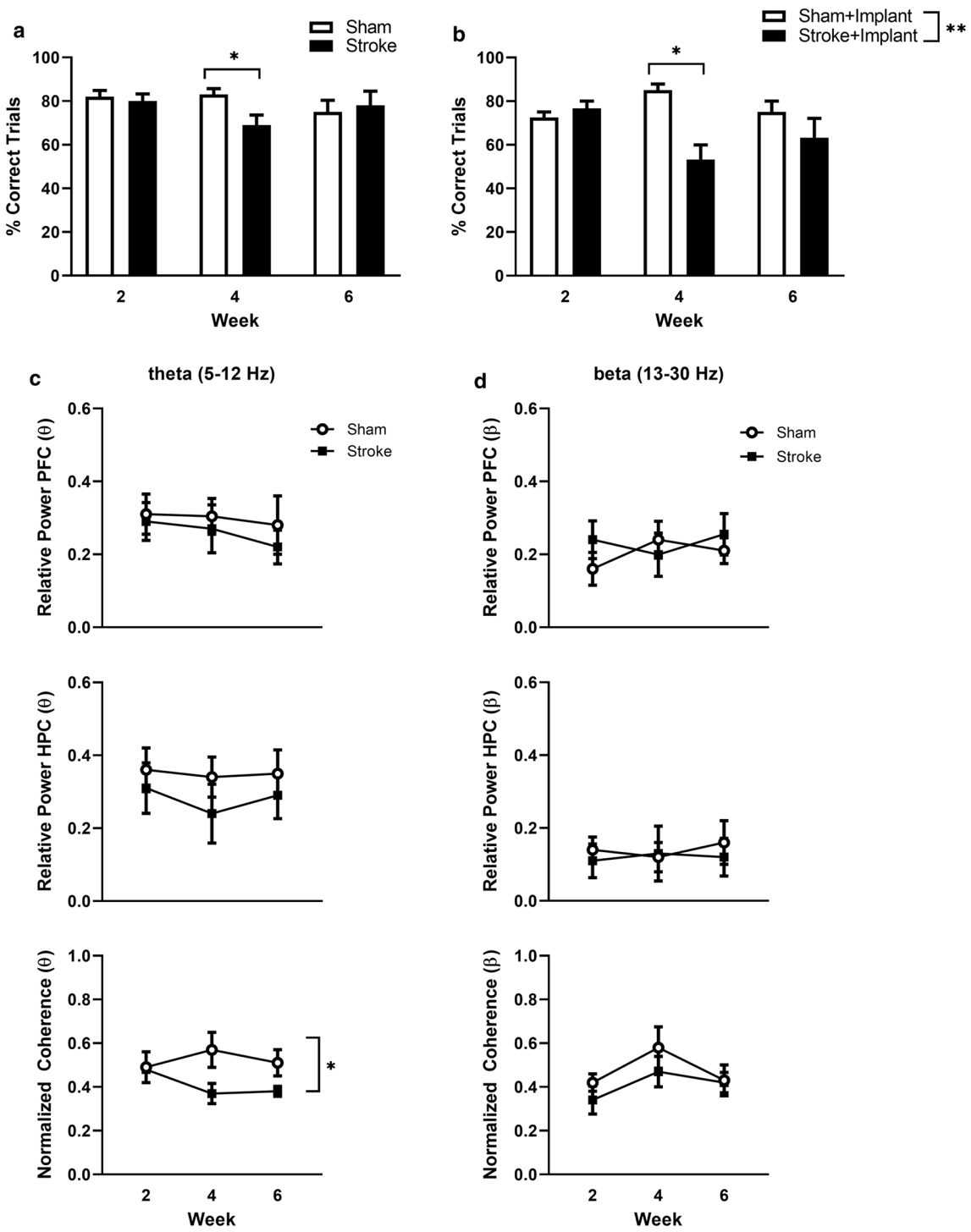

Fig. 5 Delayed non-match to sample Y-maze task. Behavioural data for **a** non-implanted animals and **b** electrode implanted animals. **c** Localised theta power in the PFC and HPC did not differ between groups or across time; however, theta coherence was significantly reduced overall in the stroke animals. **d** Localised beta power in the PFC and HPC—and oscillatory coherence between the two regions—did not differ between groups or across time. Data are shown as mean ± SEM

In line with our hypothesis, animals in the stroke group exhibited behavioural impairments in the OLR task and the Y-maze tasks as compared to sham animals. An OLR deficit in Wk 4 (but not Wk 1) was previously reported by our lab in mice (Zhou et al. 2016). In addition, an object place deficit has also been reported in rats when tested

Table 1 Correlations between task performance and normalised coherence values in the theta and beta band

	Wk 2		Wk 4		Wk 6	
	θ	β	θ	β	θ	β
OF: distance travelled	0.16	0.48	− 0.32	0.42	0.52	0.11
OLR: % displaced object	0.11	0.13	0.95**	0.77*	0.81*	0.88**
Y-maze: % correct	− 0.11	− 0.76*	0.85*	0.58	0.84*	0.44

Pearson's r values are provided, with $*p < 0.05$, $**p < 0.01$

3 weeks post-insult (Livingston-Thomas et al. 2015). Here we extend these findings by using the same task, the same task parameters, and the same animals, to map OLR performance across a 6-week time course. Of note, the OLR performance changes observed in the implanted stroke group animals from Wk 2 to Wk 4 paralleled changes in PFC–HPC theta coherence and relative PFC beta power. Animals in the stroke group exhibited a reduction in PFC–HPC theta coherence from Wk 2 to 4, and this correlated with reduced exploration of the displaced object in the test phase of the task.

A similar pattern emerged in the Y-maze delayed non-match to sample task. In Wk 2, animals in the stroke group were performing equivalent to sham animals; however, in Wk 4 a performance deficit was observed and this paralleled an observed decrease in PFC–HPC theta coherence. To our knowledge, this is the first report of a serial delayed non-match to sample Y-maze task being used in mice to assess post-stroke impairment, which we also show exhibits the same pattern of deficit as seen for the OLR spatial memory task. Endepols et al. (2015) used a one-off Y maze alternation task to assess spatial working memory in rats using the ET-1 model of stroke; however, the task parameters were markedly different (Endepols et al. 2015). In the Endepols study, rats received one free sample trial with both arms open, followed by a 1-min ITI in the home cage and a one-off test trial; this was repeated for 3 days. In our study, mice received one forced sample trial with one arm blocked, followed by a 20-s ITI in the start zone of the maze and a test trial containing food reward, which was repeated for 10 consecutive trials per session. Despite the different parameters, our findings and those reported by Endepols and colleagues both report a significant decrease in Y-maze alternation, 4 weeks post-stroke. In contrast, Livingston-Thomas et al. (2015) used an ET-1 mPFC lesion in rats and reported no post-stroke change in win/shift T-maze task performance; however, their behavioural testing spanned Wks 7–18, making it difficult to draw comparisons.

While we observed post-stroke delayed onset deficits in the Y-maze and in the OLR task in our study, the OLR deficit was more pronounced, with a significant main effect of Group across the 6 weeks. This may in part reflect exposure and training differences between the two tasks. Pre-surgery, all mice were trained to a behavioural criterion in the Y-maze task, whereas they received no OLR task exposure prior to the test session in post-stroke Wk 2. Hence spatial working memory demands needed for Y-maze performance may have been less affected post-surgery due to a degree of pre-surgery task consolidation. Of note, a significant component of recovery of function following a stroke relies on the ability to relearn tasks. Therefore, it is essential that preclinical studies establish behavioural paradigms that measure both relearning of old tasks and learning new task information, as we have undertaken with both the Y-maze and OLR task, respectively.

In a third behavioural measure, the NOR task, there were no performance differences or electrophysiological differences between the stroke and sham groups across the 6 weeks, which is in alignment with previous findings (Zhou et al. 2016). This lack of a NOR deficit supports the idea that prefrontal infarct results in specific executive dysfunctions, highlighting the need to identify and validate specific task batteries for experimental research. Here, the OLR task and Y-maze task complement each other in time course characterisation and performance in both tasks exhibited correlations to PFC–HPC theta band coherence. Taken together, these results suggest that small prefrontal infarcts produce delayed onset spatial memory impairments, and in part this may be driven by reduced theta band communication between the PFC and the HPC.

We included the OF test in our task battery as a non-spatial memory task comparator, but also because others have reported alterations in OF activity following prefrontal stroke, as well as global ischemia (Plamondon and Khan 2005). Following prefrontal stroke, increased OF locomotion has been reported in mice (Wk 1 and 4; (Zhou et al. 2016)) and rat (Wks 4, 8 and 12; (Hewlett et al. 2014)), with a further rat report citing no difference in distance travelled but decreased thigmotaxis observed in the stroke group animals (Wk 3; Livingston-Thomas et al. 2015). In contrast, Vahid-Ansari et al. reported increased thigmotaxis in mice at 10 days (2016) and 4 weeks (2018) post-stroke. Hence we wanted to characterise OF performance in our study across the 6-week time course, and also examine any between-group electrophysiological changes during this task. Similar to some of the previous reports, including our own, we observed that stroke animals travelled more distance during the 10-min OF task as compared to shams. We found no group difference in thigmotaxis at Wk 2, 4

or 6. As compared to shams, animals in the stroke group exhibited increased regional beta power in the PFC and in the HPC—and increased beta PFC–HPC coherence—in the OF, notably in Wks 2 and 4. Unlike in the spatial working memory tasks, PFC–HPC coherence (in beta or theta bands) was not correlated with the main OF behavioural metric of distance travelled.

The increases in OF locomotor activity observed in rodent models of stroke are not well understood, in terms of its behavioural interpretation and/or its underlying neural mechanisms. The electrophysiological data presented here, however, may help shed light in this area. The increased distance travelled and reduced thigmotaxis observed in post-stroke animals would generally be interpreted as increased exploratory drive and reduced anxiety, respectively (e.g. see Plamondon and Khan 2005). Indeed similar interpretations could be made from elevated plus maze experiments where animals in the stroke group exhibit increased entries into and exploration of the open arms (Plamondon and Khan 2005; Endepols et al. 2015; Hewlett et al. 2014; Zhou et al. 2016; Vahid-Ansari et al. 2016; Vahid-Ansari and Albert 2018). This appears inconsistent with human clinical data, where studies report the presence of high levels of distress in patients recovering from stroke (Hilari et al. 2010; Johnston et al. 2004). These high levels of distress show little reduction in the six month post-stroke period and are associated with poorer functional outcomes (Johnston et al. 2004). We suggest that the observed post-stroke alterations in rodent OF behaviour do not reflect reduced anxiety per se, but perhaps reflect an anxiety state of hypervigilance, an interpretation that is bolstered by the presence of high prefrontal beta power and PFC–HPC beta band coherence.

Beta band activity has been linked to top-down attention and arousal, which can be beneficial in task maintenance, however, when chronically elevated can lead to inflexible, persistence-type behaviours (Engel and Fries 2010). Moreover, frontal-parietal beta band coherence has been linked to stimulus search behaviour in monkeys (Buschman and Miller 2007). The increased OF locomotion—and elevated beta band activity—we observed in mice post-stroke could indicate high-arousal search behaviour in the arena, more reflective of the anxiety states associated with panic disorders and post-traumatic stress disorder. Indeed elevated beta band activity is observed in patients with panic disorder (de Carvalho et al. 2015) and in patients with post-traumatic stress disorder (Shim et al. 2017), and behaviourally, stroke is associated with post-traumatic stress symptomology (Bruggimann et al. 2006). Whether prefrontal stroke alters beta band activity in humans, and whether this produces an anxiety state of hypervigilance, remain unknown; however, the rodent data presented here highlights an avenue for future investigation. Others have shown in rodents that within the first week following global ischemia, OF hyperactivity can be reduced by antagonism of the hypothalamic–pituitary stress cascade (Plamondon and Khan 2006), suggesting that early stress may play a critical role in development of this hypervigilant-like behaviour.

A limitation of the current study is the small *n* for the electrophysiological experiments (stroke:sham 3:4), in part due to three exclusions for poor electrode placement but also stemming from two post-operative deaths. The combination stroke + dual electrode implant surgery was a significant surgical load for the animals and considerable post-operative care was required. Overall the implanted animals' task performance post-surgery was similar to the non-implanted groups at Wks 2, 4 and 6; however, there was a discrepancy in the Wk 2 OLR behavioural data, likely attributable to the performance of one animal and the small sample size (see Fig. 4 and "Results"). On the whole we were confident that the results obtained from the implanted mice were reflective of true group behaviour; however, replication using larger *n*'s for the electrophysiological data remains a methodological challenge.

Taken together, one interpretation of our results is that following prefrontal stroke there is a progressive remodelling process of afferent/efferent connections, including PFC–HPC connectivity. Connectivity between PFC and HPC can occur through multiple pathways, for instance via the retrosplenial cortex and thalamus (Shibata and Naito 2008). We have previously reported that changes in axonal projections / sprouting is causally linked to functional recovery after brain injury (Li et al. 2010; Overman et al. 2012; Clarkson et al. 2013). In addition, we have recently shown that prefrontal stroke induces a progressive loss of connections between the PFC and thalamus (Barwick et al. 2018), which represents a potential underlying mechanism for the delayed impairment in spatial memory and altered PFC–HPC connectivity. A likely trigger for this progressive loss of connections is a prolonged increase in reactive astrogliosis in white matter tracts, which has been reported in both post-mortem human brains and animal models, and correlated with delayed cognitive impairments (Chen et al. 2016; Hase et al. 2018). Here we add to these findings by demonstrating functional connectivity changes in PFC–HPC communication in the 6 weeks following infarct to the PFC. In particular, a delayed drop in PFC–HPC functional connectivity parallels a drop in spatial working memory performance, as evidenced in the OLR and Y-maze tasks. Additionally, we report changes in intra- and inter-regional beta band activity in the OF, which may reflect a hypervigilant state in the OF arena. Lastly, of excitement but preliminary in nature, we report that following PFC infarct, early open field changes in PFC beta band power correlate to later-stage spatial memory impairments, highlighting this as a potential biomarker for detecting when spatial memory impairments are likely to occur.

Acknowledgements This project was supported by Marsden Grant #UOO1407 administered by The Royal Society of New Zealand.

Compliance with Ethical Standards

Conflict of interest The authors confirm that there are no conflicts of interest in the present research.

Ethical Approval All experimental protocols were approved by the University of Otago Animal Ethics Committee (AEC Protocol 13/15), which adheres to the New Zealand Animal Welfare Act 1999. All procedures were carried out in accordance with the ARRIVE guidelines with mice being assigned to either stroke or sham experimental groups at the time of surgery by one member of staff, ensuring all behavioural and electrophysiological procedures were undertaken in a blind manner.

References

Barwick, D. K., Joy, M. T., Gowing, E. K., Carmichael, S. T., & Clarkson, A. N. (2018). Identifying changes in axonal connectivity following prefrontal cortex stroke in mice: Impaired thalamic input. In *10th International Symposium on Neuroprotection and Neurorepair (ISN&N)*, Dresden, Germany, 17th–20th October, 2018.

Benchenane, K., Peyrache, A., Khamassi, M., Tierney, P. L., Gioanni, Y., Battaglia, F. P., et al. (2010). Coherent theta oscillations and reorganization of spike timing in the hippocampal-prefrontal network upon learning. *Neuron, 66*(6), 921–936. https://doi.org/10.1016/j.neuron.2010.05.013.

Brincat, S. L., & Miller, E. K. (2015). Frequency-specific hippocampal-prefrontal interactions during associative learning. *Nature Neuroscience, 18*(4), 576. https://doi.org/10.1038/nn.3954.

Bruggimann, L., Annoni, J. M., Staub, F., von Steinbuchel, N., Van der Linden, M., & Bogousslavsky, J. (2006). Chronic posttraumatic stress symptoms after nonsevere stroke. *Neurology, 66*(4), 513–516. https://doi.org/10.1212/01.wnl.0000194210.98757.49.

Buschman, T. J., & Miller, E. K. (2007). Top-down versus bottom-up control of attention in the prefrontal and posterior parietal cortices. *Science, 315*(5820), 1860–1862. https://doi.org/10.1126/science.1138071.

Chen, A., Akinyemi, R. O., Hase, Y., Firbank, M. J., Ndung'u, M. N., Foster, V., et al. (2016). Frontal white matter hyperintensities, clasmatodendrosis and gliovascular abnormalities in ageing and post-stroke dementia. *Brain, 139*(Pt 1), 242–258. https://doi.org/10.1093/brain/awv328.

Clarkson, A. N., Lopez-Valdes, H. E., Overman, J. J., Charles, A. C., Brennan, K. C., & Thomas Carmichael, S. (2013). Multimodal examination of structural and functional remapping in the mouse photothrombotic stroke model. *Journal of Cerebral Blood Flow and Metabolism, 33*(5), 716–723. https://doi.org/10.1038/jcbfm.2013.7.

Colgin, L. L. (2011). Oscillations and hippocampal-prefrontal synchrony. *Current Opinion in Neurobiology, 21*(3), 467–474. https://doi.org/10.1016/j.conb.2011.04.006.

Cordova, C. A., Jackson, D., Langdon, K. D., Hewlett, K. A., & Corbett, D. (2014). Impaired executive function following ischemic stroke in the rat medial prefrontal cortex. *Behavioural Brain Research, 258,* 106–111. https://doi.org/10.1016/j.bbr.2013.10.022.

de Carvalho, M. R., Velasques, B. B., Freire, R. C., Cagy, M., Marques, J. B., Teixeira, S., et al. (2015). Frontal cortex absolute beta power measurement in Panic Disorder with Agoraphobia patients. *Journal of Affective Disorders, 184,* 176–181. https://doi.org/10.1016/j.jad.2015.05.055.

Deziel, R. A., Ryan, C. L., & Tasker, R. A. (2015). Ischemic lesions localized to the medial prefrontal cortex produce selective deficits in measures of executive function in rats. *Behavioural Brain Research, 293,* 54–61. https://doi.org/10.1016/j.bbr.2015.07.003.

Endepols, H., Mertgens, H., Backes, H., Himmelreich, U., Neumaier, B., Graf, R., et al. (2015). Longitudinal assessment of infarct progression, brain metabolism and behavior following anterior cerebral artery occlusion in rats. *Journal of Neuroscience Methods, 253,* 279–291. https://doi.org/10.1016/j.jneumeth.2014.11.003.

Engel, A. K., & Fries, P. (2010). Beta-band oscillations—Signalling the status quo? *Current Opinion in Neurobiology, 20*(2), 156–165. https://doi.org/10.1016/j.conb.2010.02.015.

Franklin, K., & Paxinos, G. (2008). *The mouse brain in stereotaxic coordinates*. San Diego: Academic Press.

Griffin, A. L. (2015). Role of the thalamic nucleus reuniens in mediating interactions between the hippocampus and medial prefrontal cortex during spatial working memory. *Frontiers in Systems Neuroscience, 9,* 29. https://doi.org/10.3389/fnsys.2015.00029.

Hachinski, V., Iadecola, C., Petersen, R. C., Breteler, M. M., Nyenhuis, D. L., Black, S. E., et al. (2006). National Institute of Neurological Disorders and Stroke-Canadian Stroke Network vascular cognitive impairment harmonization standards. *Stroke, 37*(9), 2220–2241. https://doi.org/10.1161/01.STR.0000237236.88823.47.

Hase, Y., Craggs, L., Hase, M., Stevenson, W., Slade, J., Chen, A., et al. (2018). The effects of environmental enrichment on white matter pathology in a mouse model of chronic cerebral hypoperfusion. *Journal of Cerebral Blood Flow and Metabolism, 38*(1), 151–165. https://doi.org/10.1177/0271678X17694904.

Hewlett, K. A., Kelly, M. H., & Corbett, D. (2014). 'Not-so-minor' stroke: Lasting psychosocial consequences of anterior cingulate cortical ischemia in the rat. *Experimental Neurology, 261,* 543–550. https://doi.org/10.1016/j.expneurol.2014.07.024.

Hilari, K., Northcott, S., Roy, P., Marshall, J., Wiggins, R. D., Chataway, J., et al. (2010). Psychological distress after stroke and aphasia: The first six months. *Clinical Rehabilitation, 24*(2), 181–190. https://doi.org/10.1177/0269215509346090.

Hillman, K. L., & Bilkey, D. K. (2010). Neurons in the rat anterior cingulate cortex dynamically encode cost-benefit in a spatial decision-making task. *Journal of Neuroscience, 30*(22), 7705–7713. https://doi.org/10.1523/JNEUROSCI.1273-10.2010.

Houlton, J., Zhou, L. Y. Y., Barwick, D., Gowing, E. K., & Clarkson, A. N. (2019). Stroke induces a BDNF-dependent improvement in cognitive flexibility in aged mice. *Neural Plasticity, 5*(2019), 1460890. https://doi.org/10.1155/2019/1460890.

Hyman, J. M., Zilli, E. A., Paley, A. M., & Hasselmo, M. E. (2010). Working memory performance correlates with prefrontal-hippocampal theta interactions but not with prefrontal neuron firing rates. *Frontiers in Integrative Neuroscience, 4,* 2. https://doi.org/10.3389/neuro.07.002.2010.

Johnston, M., Pollard, B., Morrison, V., & MacWalter, R. (2004). Functional limitations and survival following stroke: Psychological and clinical predictors of 3-year outcome. *International Journal of Behavioral Medicine, 11*(4), 187–196. https://doi.org/10.1207/s15327558ijbm1104_1.

Jones, M. W., & Wilson, M. A. (2005). Theta rhythms coordinate hippocampal-prefrontal interactions in a spatial memory task. *PLoS Biology, 3*(12), e402. https://doi.org/10.1371/journal.pbio.0030402.

Levine, D. A., Galecki, A. T., Langa, K. M., Unverzagt, F. W., Kabeto, M. U., Giordani, B., et al. (2015). Trajectory of cognitive decline after incident stroke. *JAMA, 314*(1), 41–51. https://doi.org/10.1001/jama.2015.6968.

Li, S., Overman, J. J., Katsman, D., Kozlov, S. V., Donnelly, C. J., Twiss, J. L., et al. (2010). An age-related sprouting transcriptome

provides molecular control of axonal sprouting after stroke. *Nature Neuroscience, 13*(12), 1496–1504. https://doi.org/10.1038/nn.2674.

Livingston-Thomas, J. M., Jeffers, M. S., Nguemeni, C., Shoichet, M. S., Morshead, C. M., & Corbett, D. (2015). Assessing cognitive function following medial prefrontal stroke in the rat. *Behavioural Brain Research, 294,* 102–110. https://doi.org/10.1016/j.bbr.2015.07.053.

Loeb, C., Gandolfo, C., Croce, R., & Conti, M. (1992). Dementia associated with lacunar infarction. *Stroke, 23*(9), 1225–1229.

Lundqvist, M., Rose, J., Herman, P., Brincat, S. L., Buschman, T. J., & Miller, E. K. (2016). Gamma and beta bursts underlie working memory. *Neuron, 90*(1), 152–164. https://doi.org/10.1016/j.neuron.2016.02.028.

Moorhouse, P., & Rockwood, K. (2008). Vascular cognitive impairment: Current concepts and clinical developments. *The Lancet Neurology, 7*(3), 246–255. https://doi.org/10.1016/S1474-4422(08)70040-1.

O'Brien, J. T., Erkinjuntti, T., Reisberg, B., Roman, G., Sawada, T., Pantoni, L., et al. (2003). Vascular cognitive impairment. *The Lancet Neurology, 2*(2), 89–98.

O'Neill, P. K., Gordon, J. A., & Sigurdsson, T. (2013). Theta oscillations in the medial prefrontal cortex are modulated by spatial working memory and synchronize with the hippocampus through its ventral subregion. *Journal of Neuroscience, 33*(35), 14211–14224. https://doi.org/10.1523/JNEUROSCI.2378-13.2013.

Overman, J. J., Clarkson, A. N., Wanner, I. B., Overman, W. T., Eckstein, I., Maguire, J. L., et al. (2012). A role for ephrin-A5 in axonal sprouting, recovery, and activity-dependent plasticity after stroke. *Proceedings of the National academy of Sciences of the United States of America, 109*(33), E2230–2239. https://doi.org/10.1073/pnas.1204386109.

Patel, M. D., Coshall, C., Rudd, A. G., & Wolfe, C. D. (2002). Cognitive impairment after stroke: Clinical determinants and its associations with long-term stroke outcomes. *Journal of the American Geriatrics Society, 50*(4), 700–706.

Petersen, R. C. (2004). Mild cognitive impairment as a diagnostic entity. *Journal of Internal Medicine, 256*(3), 183–194. https://doi.org/10.1111/j.1365-2796.2004.01388.x.

Plamondon, H., & Khan, S. (2005). Characterization of anxiety and habituation profile following global ischemia in rats. *Physiology & Behavior, 84*(4), 543–552. https://doi.org/10.1016/j.physbeh.2005.02.001.

Plamondon, H., & Khan, S. (2006). The CRH1 antagonist CP154,526 failed to alter ischemia-induced neurodegeneration and spatial memory deficits in rats but inhibited behavioral activity in the novel open field. *Behavioural Brain Research, 166*(1), 85–92. https://doi.org/10.1016/j.bbr.2005.07.031.

Rodriguez Garcia, P. L., & Rodriguez Garcia, D. (2015). Diagnosis of vascular cognitive impairment and its main categories. *Neurologia, 30*(4), 223–239. https://doi.org/10.1016/j.nrl.2011.12.014.

Shibata, H., & Naito, J. (2008). Organization of anterior cingulate and frontal cortical projections to the retrosplenial cortex in the rat. *Journal of Comparative Neurology, 506*(1), 30–45. https://doi.org/10.1002/cne.21523.

Shim, M., Im, C. H., & Lee, S. H. (2017). Disrupted cortical brain network in post-traumatic stress disorder patients: A resting-state electroencephalographic study. *Translational Psychiatry, 7*(9), e1231. https://doi.org/10.1038/tp.2017.200.

Tatemichi, T. K., Desmond, D. W., Stern, Y., Paik, M., Sano, M., & Bagiella, E. (1994). Cognitive impairment after stroke: Frequency, patterns, and relationship to functional abilities. *Journal of Neurology, Neurosurgery and Psychiatry, 57*(2), 202–207.

Vahid-Ansari, F., & Albert, P. R. (2018). Chronic fluoxetine induces activity changes in recovery from poststroke anxiety, depression, and cognitive impairment. *Neurotherapeutics, 15*(1), 200–215. https://doi.org/10.1007/s13311-017-0590-3.

Vahid-Ansari, F., Lagace, D. C., & Albert, P. R. (2016). Persistent post-stroke depression in mice following unilateral medial prefrontal cortical stroke. *Translational Psychiatry, 6*(8), e863. https://doi.org/10.1038/tp.2016.124.

Vermeer, S. E., Longstreth, W. T., Jr., & Koudstaal, P. J. (2007). Silent brain infarcts: A systematic review. *The Lancet Neurology, 6*(7), 611–619. https://doi.org/10.1016/S1474-4422(07)70170-9.

Zhou, L. Y. Y., Wright, T. E., & Clarkson, A. N. (2016). Prefrontal cortex stroke induces delayed impairment in spatial memory. *Behavioural Brain Research, 296,* 373–378. https://doi.org/10.1016/j.bbr.2015.08.022.